

# An interference-free and rapid electrochemical lateral-flow immunoassay for one-step ultrasensitive detection with serum†

Cite this: DOI: 10.1039/c3an02328a

Md. Rajibul Akanda,<sup>a</sup> Hyou-Arm Joung,<sup>b</sup> Vellaiappillai Tamilavan,<sup>a</sup> Seonhwa Park,<sup>a</sup> Sinyoung Kim,<sup>c</sup> Myung Ho Hyun,<sup>a</sup> Min-Gon Kim<sup>\*b</sup> and Haesik Yang<sup>\*a</sup>

Point-of-care testing (POCT) of biomarkers in clinical samples is of great importance for rapid and cost-effective diagnosis. However, it is extremely challenging to develop an electrochemical POCT technique retaining both ultrasensitivity and simplicity. We report an interference-free electrochemical lateral-flow immunoassay that enables one-step ultrasensitive detection with serum. The electrochemical-chemical (ECC) redox cycling combined with an enzymatic reaction of an enzyme label is used to obtain high signal amplification. The ECC redox cycling involving  $\text{Ru}(\text{NH}_3)_6^{3+}$ , enzyme product, and tris(3-carboxyethyl)phosphine (TCEP) depends on pH, because the formal potential of an enzyme product and TCEP increases with decreasing pH although that of  $\text{Ru}(\text{NH}_3)_6^{3+}$  is pH-independent. With consideration of the pH dependence of ECC redox cycling, a noble combination of enzyme label, substrate, and product [ $\beta$ -galactosidase, 4-amino-1-naphthyl  $\beta$ -D-galactopyranoside, and 4-amino-1-naphthol, respectively] is introduced to ensure fast and selective ECC redox cycling of the enzyme product along with a low background level. The selective ECC redox cycling at a low applied potential (0.05 V vs. Ag/AgCl) minimizes the interference effect of electroactive species (L-ascorbic acid, acetaminophen, and uric acid) in serum. A detection limit of 0.1 pg mL<sup>-1</sup> for troponin I is obtained only 11 min after serum dropping without the use of an additional solution. Moreover, the lateral-flow immunoassay is applicable to the analysis of real clinical samples.

Received 17th December 2013  
Accepted 2nd January 2014

DOI: 10.1039/c3an02328a

www.rsc.org/analyst

## Introduction

Immunoassays using affinity binding between antigen and antibody have been widely used in bioassays because of their high sensitivity and selectivity. In recent years, point-of-care testing (POCT) of biomarkers in clinical samples is of great importance for rapid and cost-effective diagnosis.<sup>1–3</sup> Though a number of immunoassays utilizing lateral-flow strips,<sup>4,5</sup> lab-on-a-chip,<sup>6,7</sup> and paper-based devices<sup>8,9</sup> have been developed to this end, many of them have limitations in terms of simplicity, rapidness, cost-effectiveness and ultrasensitivity. It is extremely challenging to develop an ultrasensitive technique retaining simplicity.

A number of immunoassays are in practice, wherein the simplicity is significantly affected by the number of solutions

used in the process. In general sandwich-type immunoassays, a washing solution, in addition to a sample solution, is used to remove interfering unbound labeled probes. Interestingly, in optical lateral-flow immunoassays employing highly light-absorbing or fluorescent labels, continuous flow of a sample solution removes the unbound labeled probes, thereby eliminating the need for a washing solution.<sup>5,10,11</sup> Nevertheless, in many cases, these simple immunoassays have limited sensitivities and lack of quantitative analysis. Though signal amplification by enzyme labels has been frequently introduced in lateral-flow immunoassays, it is not sufficient for obtaining ultrasensitivity.<sup>4,12</sup> Moreover, in most cases, simplicity is compromised because of the requirement of an appropriate supply of an additional solution containing the enzyme substrate.<sup>4,12</sup> In electrochemical lateral-flow immunoassays, which are employed to construct miniaturized POCT devices, the presence of interfering electroactive species like L-ascorbic acid (AA) in serum always necessitates the use of an additional interference-free solution,<sup>13</sup> thereby enhancing the complexity of the procedure. To improve sensitivity without compromising on simplicity, a long incubation period can be used in both antigen-antibody binding and enzymatic reactions. However, rapid solution evaporation in lateral-flow immunoassays renders the application of a long incubation period incompatible. Hence, it

<sup>a</sup>Department of Chemistry and Chemistry Institute for Functional Materials, Pusan National University, Busan 609-735, Korea. E-mail: hyang@pusan.ac.kr

<sup>b</sup>School of Physics and Chemistry, Gwangju Institute of Science and Technology (GIST), Gwangju 500-712, Korea. E-mail: mkim@gist.ac.kr

<sup>c</sup>Department of Laboratory Medicine, Yonsei University College of Medicine, Seoul 135-720, Korea

† Electronic supplementary information (ESI) available: More supplementary data. See DOI: 10.1039/c3an02328a



After the photoresist-coated plates were soft-baked, the plates were exposed to UV light in a mask aligner equipped with a patterned mask. The exposed plates were developed and hard-baked. The baked plates were immersed into an ITO-etching solution. Afterward, the remaining photoresist was removed with acetone. The patterned ITO glass substrates were diced into smaller sections. The diced substrates were sequentially cleaned with trichloroethylene, ethanol, and distilled water under sonication for 15 min. The cleaned substrates were pre-treated with a solution of 5 : 1 : 1 H<sub>2</sub>O–H<sub>2</sub>O<sub>2</sub> (30%)–NH<sub>4</sub>OH (30%) at 70 °C for 1.5 h. To fabricate a reference electrode and a counter electrode on the patterned ITO electrodes, Ag/AgCl ink (ALS, 011464) and Ag paste were selectively dropped on the patterned electrodes. Finally, the substrates were dried at 70 °C.

### Fabrication of lateral-flow immunostrips

The preparation and performance of lateral-flow immunostrips were reported previously.<sup>20,22</sup> The nitrocellulose membrane was obtained from Millipore (HFB02404; Billerica, MA). The sample pad (P/N BSP-133-20) and asymmetric polysulfone membrane (ASPM, Vivid plasma separation-GX, USA) were obtained from Pall Co. (Port Washington, NY). A sample pad (5 mm × 20 mm) and an absorbent pad (5 mm × 20 mm) were attached to a nitrocellulose membrane (5 mm × 60 mm). 1 μL of PBS buffer containing 1 mg mL<sup>-1</sup> antitroponin-I IgG (capture IgG) was dropped and dried on the nitrocellulose membrane near the working electrode, and 5 μL of PBSB buffer containing 1 μg mL<sup>-1</sup> Gal-conjugated antitroponin-I IgG (detection probe), 2% surfactant, and 2% PVP was dropped and dried on the nitrocellulose membrane 1 cm apart from the capture IgG-dropped region. To detect IgG readily dissolved during the flow of sample solution, surfactant and PVP were used. An asymmetric membrane pad<sup>20</sup> (5 mm × 5 mm) was placed on the nitrocellulose membrane 0.5 cm apart from the Gal-conjugated IgG-dropped region (see Fig. 1b). A substrate pad (5 mm × 5 mm) was immersed in PBS buffer containing 30 mM Ru(NH<sub>3</sub>)<sub>6</sub><sup>3+</sup>, 15 mM AN-GP, and 60 mM TCEP. After the substrate pad was dried, it was placed on the asymmetric membrane pad (see Fig. 1b). The assembly of the substrate pad, the asymmetric membrane pad, and the nitrocellulose membrane was tightly bound by winding a scotch tape around the assembly. The asymmetric membrane pad has asymmetric pore sizes: the pore size gradually increases from one side to the other side.<sup>20,22</sup> The smaller pore side is in contact with the nitrocellulose membrane. The asymmetric membrane pad is slowly vertically wetted due to unfavorable capillary action from the smaller pore to the larger pore, and the substrates in the substrate pad are then dissolved and released. It allows delayed release of the substrates into the nitrocellulose membrane. The glass plate containing a micropatterned ITO working electrode, an Ag/AgCl reference electrode, and an Ag counter electrode was placed on the nitrocellulose membrane (see Fig. 1b). To ensure tight contact, the membrane and the glass substrate were clamped. The area of the working electrode in contact with the nitrocellulose membrane was 10 mm<sup>2</sup> (2 mm × 5 mm), and the distance between the working electrode and reference electrode

and between the reference electrode and counter electrode was 3 mm. Electrochemical measurements were carried out using a CHI 405A or CHI 708C (CH Instruments, Austin, TX, USA). All electrochemical measurements except those using electrochemical lateral-flow immunostrips were performed using a Teflon electrochemical cell consisting of an ITO working electrode, an Ag/AgCl (3 M NaCl) reference electrode, and a platinum counter electrode. The exposed area of each ITO electrode was ca. 0.28 cm<sup>2</sup>. All immunostrip experiments were carried out at room temperature. Troponin I in real clinical samples was measured on a Beckman Coulter Access 2 analyzer with enhanced AccuTnI reagent (Reagent part number A78803, Beckman Coulter Diagnostics, Brea, CA, USA). The study protocol using real clinical samples was approved by the Institutional Review Board of Gangnam Severance Hospitals (#3-2011-0284) and complies with the Declaration of Helsinki.

## Results and discussion

In our previous reports, ECC redox cycling was carried out in Tris buffer containing 2.0 mM TCEP (pH 8.9).<sup>16,17</sup> Under these conditions, ECC redox cycling of both AP and HQ was fast, as shown in the chronocoulograms in Fig. 2a; the charge in the presence of AP or HQ (curve ii or iii in Fig. 2a) was considerably higher than that in their absence (curve i in Fig. 2a). In order to validate the applicability of ECC redox cycling in serum containing TCEP, we investigated this in serum-like PBS solution containing 2.0 mM TCEP (ca. pH 6.0). Because TCEP hydrochloride is mixed with serum, the pH of serum containing TCEP becomes less than the pH of serum (7.4). Accordingly, ECC redox cycling was investigated in pH 6.0. Strikingly, ECC redox cycling of both AP and HQ was very slow, with no significant difference between the charges in the presence (curve ii or iii in Fig. 2b) and absence (curve i in Fig. 2b) of AP or HQ. Hence, we found that AP and HQ were unsuitable for fast ECC redox cycling in serum containing TCEP. Cyclic voltammograms in Fig. S1a and S1b of the ESI† also confirm that ECC redox cycling of both AP and HQ was inefficient at pH 6.0.

Fig. 3a shows the relative levels of the applied electrode potential and the formal potential of three redox couples participating in ECC redox cycling. The formal potential of

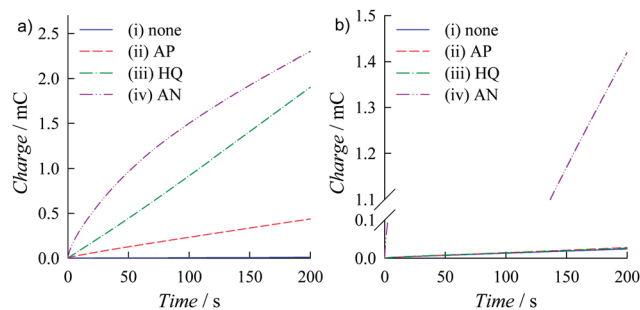
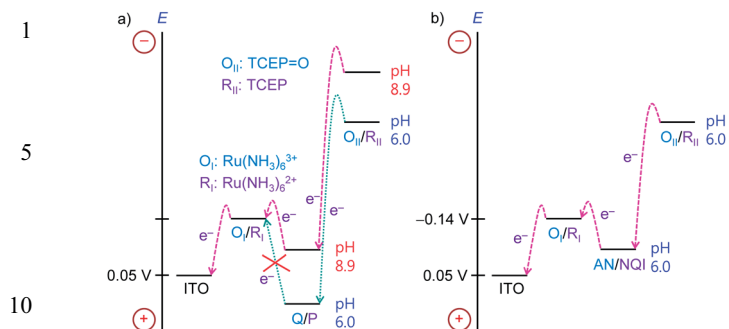


Fig. 2 Chronocoulograms obtained at 0.05 V at ITO electrodes in (a) Tris buffer (pH 8.9); (b) PBS buffer (pH 6.0) containing 1.0 mM Ru(NH<sub>3</sub>)<sub>6</sub><sup>3+</sup> and 2.0 mM TCEP: (i) no reactant, (ii) 0.1 mM 4-aminophenol (AP), (iii) 0.1 mM hydroquinone (HQ), or (iv) 0.1 mM AN.



**Fig. 3** Schematic of the relative levels of the applied electrode potential and the formal potential (in pH 8.9 and 6.0) of the three redox couples participating in ECC redox cycling. The arrows represent possible electron-transfer reactions between redox species. (a) Representation of ECC redox cycling of P; where P and Q refer to AP (or HQ) and the oxidized form of AP (or the oxidized form of HQ), respectively. (b) Representation of ECC redox cycling of AN.

$\text{Ru}(\text{NH}_3)_6^{3+}/\text{Ru}(\text{NH}_3)_6^{2+}$  is pH-independent, whereas the formal potential of Q/P and TCEP=O (the oxidized form of TCEP)/TCEP increases with decreasing pH. Therefore, ECC redox cycling highly depends on pH. At pH 8.9, the endergonic reaction between  $\text{Ru}(\text{NH}_3)_6^{3+}$  and P (AP or HQ) is driven by the highly exergonic reaction between TCEP and Q (the oxidized form of AP or HQ) *via* a coupled reaction mechanism.<sup>16</sup> At pH 6.0, however, the endergonic reaction between  $\text{Ru}(\text{NH}_3)_6^{3+}$  and P is less favored than at pH 8.9, because of the larger difference in the formal potential between the two redox couples [ $\text{Ru}(\text{NH}_3)_6^{3+}/\text{Ru}(\text{NH}_3)_6^{2+}$  and Q/P], resulting in slow ECC redox cycling of AP or HQ at pH 6.0.

The formal potential of AN is lower than those of AP and HQ and is closer to that of  $\text{Ru}(\text{NH}_3)_6^{3+}$  at pH 6.0 (Fig. 3b). This favors efficient ECC redox cycling at both pH 6.0 and 8.9 because of the small difference in the formal potential between AN and  $\text{Ru}(\text{NH}_3)_6^{3+}$ , as indicated by higher charges in the presence of AN (curve iv in Fig. 2a and b) than in the absence of AN (curve i in Fig. 2a and b). Cyclic voltammograms in Fig. S1c of the ESI† also confirm fast ECC redox cycling at pH 6.0. The applied potential for ECC redox cycling should be optimized to obtain high signal-to-background ratios by minimizing the electro-reduction (electrooxidation) of  $\text{Ru}(\text{NH}_3)_6^{3+}$  to  $\text{Ru}(\text{NH}_3)_6^{2+}$  ( $\text{Ru}^{\text{IV}}$  complex).<sup>16,23,24</sup> In the ECC redox cycling of AN (i of Fig. 1a), an applied potential of 0.05 V was found to be optimal (see Fig. S2 of the ESI†).

The background levels obtained in serum with the electrochemical immunoassay using ECC redox cycling of AN can be affected by (i) ECC redox cycling (ii of Fig. 1a), (ii) electrochemical-chemical (EC) redox cycling of interfering electroactive species (iii of Fig. 1a), and (iii) ECC redox cycling of AN-GP (Fig. S3†). The EC redox cycling includes direct electrooxidation of interfering species. Several interfering electroactive species, for example, AA, uric acid, and acetaminophen, are present in human serum,<sup>25</sup> and their concentrations vary with the sample type and time. Cyclic voltammograms of PBS buffer, both in the absence (curve i in Fig. 4a) and presence of TCEP (curve ii in Fig. 4a), did not show significant anodic (faradaic) current.

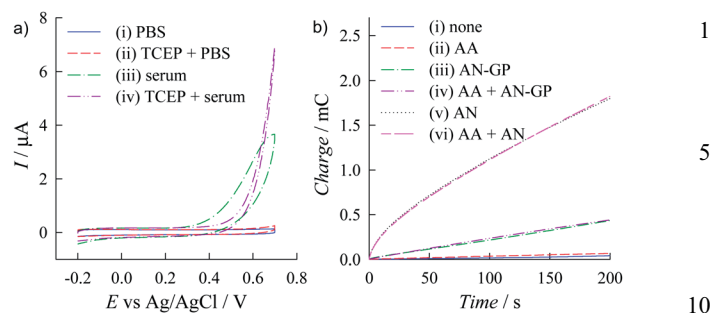


**Fig. 4** (a) Cyclic voltammograms obtained at bare ITO electrodes in either (i) PBS (pH 7.4), (ii) PBS containing 2.0 mM TCEP (pH 6.0), (iii) serum, or (iv) serum containing 2.0 mM TCEP. (b) Chronocoulograms obtained at 0.05 V at ITO electrodes in PBS buffer (pH 6.0) containing 1.0 mM  $\text{Ru}(\text{NH}_3)_6^{3+}$  and 2.0 mM TCEP: (i) no reactant, (ii) 0.1 mM AA, (iii) 1.0 mM AN-GP, (iv) 0.1 mM AA and 1.0 mM AN-GP, (v) 0.1 mM AN, or (vi) 0.1 mM AA and 0.1 mM AN.

However, a high anodic current was observed above 0.3 V in serum without (curve iii in Fig. 4a) and with (curve iv in Fig. 4a) TCEP, indicating the presence of interfering electroactive species. The applied potential of 0.05 V, which is significantly lower than the anodic current-generating potential, is suitable for the minimization of direct electrooxidation of interfering species. It is also reported that direct electrooxidation of interfering species is negligible at potentials close to 0 V.<sup>25</sup> Nevertheless, the ECC redox cycling of interfering species cannot be ruled out completely. When the charge in a solution containing AA,  $\text{Ru}(\text{NH}_3)_6^{3+}$ , and TCEP (curve ii in Fig. 4b) was compared to that in a solution containing  $\text{Ru}(\text{NH}_3)_6^{3+}$  and TCEP (curve i in Fig. 4b), the former was higher than the latter, indicating the occurrence of undesired ECC and EC redox cycling of AA. However, the charge in the AA solution (curve ii in Fig. 4b) was significantly lower than that in an AN solution (curve v in Fig. 4b), which signifies that ECC and EC redox cycling of AA are much slower than ECC redox cycling of AN. This can be attributed to the slow reaction between AA and  $\text{Ru}(\text{NH}_3)_6^{3+}$  (ii of Fig. 1a) and slow oxidation of AA at the ITO electrode (iii of Fig. 1a), considering fast reduction of the oxidized form of AA by TCEP.<sup>26</sup> All results indicate that the background levels were dominated by AN-GP rather than AA.

Slow ECC redox cycling of the enzyme substrate (AN-GP) (Fig. S3†) is a requisite for obtaining low background levels.<sup>17</sup> Voltammograms indicate the presence of higher charge in a solution containing AN-GP,  $\text{Ru}(\text{NH}_3)_6^{3+}$ , and TCEP (curve iii in Fig. 4b) as compared to a solution containing  $\text{Ru}(\text{NH}_3)_6^{3+}$  and TCEP (curve i in Fig. 4b). The AN-GP solution contains lower charge than a 10-fold dilute AN solution (curve v in Fig. 4b), confirming that the ECC redox cycling of AN-GP is much slower than that of AN. Our data reveal the presence of similar charge in solutions containing AN-GP,  $\text{Ru}(\text{NH}_3)_6^{3+}$  and TCEP, in the presence (curve iv in Fig. 4b) and absence of AA (curve iii in Fig. 4b). Similar results were also obtained in solutions containing AN,  $\text{Ru}(\text{NH}_3)_6^{3+}$ , and TCEP, with (curve vi in Fig. 4b) and without AA (curve v in Fig. 4b). These results clearly demonstrate the negligible interference effect of AA in both signal and

background levels, in addition to a smaller contribution of the ECC and EC redox cycling of AA to the background level than that of AN-GP. This, in general, implies that sample- and time-dependent variations in the AA concentration do not affect signal and background levels significantly. Moreover, a relatively higher contribution of AN-GP to the background level does not pose a serious problem because of its high reproducibility. The interference effects in the case of uric acid and acetaminophen were also found to be negligible (see Fig. S4 in the ESI†).

The lateral-flow immunoassay using ECC redox cycling of AN was employed for detection of troponin I in human serum (Fig. 1). Gal was used as an enzyme label for signal amplification to avoid interference with ALP present in blood serum. Gal converted AN-GP into AN, which in turn triggered chemical-chemical redox cycling of AN during the incubation period. Fast ECC redox cycling of AN was induced on the application of a potential of 0.05 V at a bare ITO working electrode. A substrate pad dipped in a solution containing AN-GP,  $\text{Ru}(\text{NH}_3)_6^{3+}$  and TCEP was dried and subsequently attached to an asymmetric membrane pad on a nitrocellulose membrane (Fig. 1b). Capture IgG was immobilized on the membrane to which a patterned ITO working electrode was attached. Gal-conjugated detection IgG was dropped onto the middle of the membrane. 120  $\mu\text{L}$  of serum, spiked with troponin I, was dropped on a sample pad, followed by a capillary-driven flow of serum from the sample pad to the absorbent pad. During the flow, troponin I bound to Gal-conjugate IgG and then to capture IgG. The asymmetric membrane pad was slowly wetted, and AN-GP,  $\text{Ru}(\text{NH}_3)_6^{3+}$ , and TCEP in the substrate pad were released with a time delay and transferred to the absorbent pad<sup>20</sup> (refer to the animation in the ESI†). This was followed by an enzymatic reaction and redox cycling after unbound Gal-conjugated detection IgGs were washed to suppress their enzymatic reactions. The photograph of an assembled immunostrip is shown in Fig. S5 of the ESI.† Chronocoulograms were measured at 10 min after serum dropping.

The chronocoulograms in Fig. 5a, obtained with the electrochemical lateral-flow immunostrips, indicate an increase in charge with increasing concentrations of troponin I spiked in troponin I-free human serum. Fig. 5b presents a calibration plot obtained from the charge data recorded at 60 s in the chronocoulogram. The calculated detection limit for troponin I was 0.1  $\text{pg mL}^{-1}$ , which is the lowest reported value in lateral-flow immunoassays to date.<sup>11,27–29</sup> Moreover, troponin I was detected over a wide range of concentrations from 0.1  $\text{pg mL}^{-1}$  to 100  $\text{ng mL}^{-1}$ .

To investigate the effect of interference in the lateral-flow immunoassay, chronocoulograms were obtained with serum containing AA and ALP (Fig. 5c). At both concentrations of troponin I (0 and 1  $\text{pg mL}^{-1}$ ), the chronocoulograms in the presence of AA and ALP (curve ii or iv in Fig. 5c) were similar to those in their absence (curve i or iii in Fig. 5c, respectively). This result reconfirms the negligible interference of AA and ALP in the immunoassay. The lateral-flow immunoassay was also tested with a standard reference material from NIST, containing troponin I, troponin T, and troponin C. As illustrated in Fig. 5d,

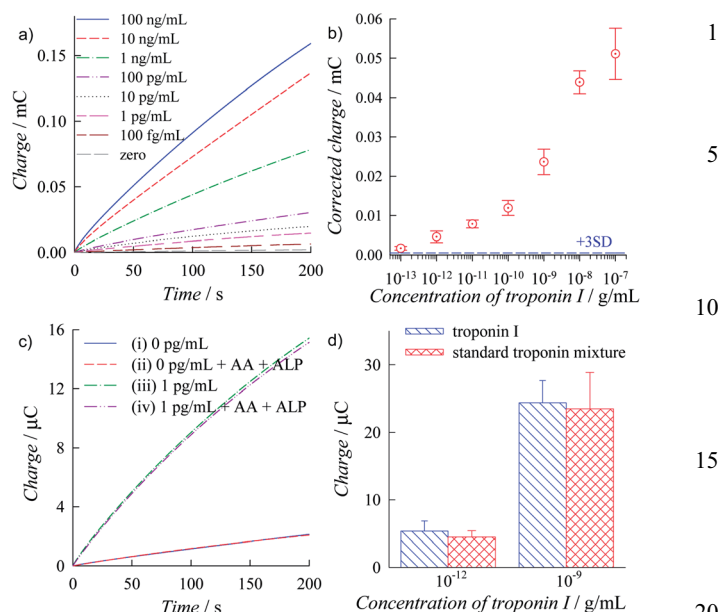


Fig. 5 (a) Chronocoulograms obtained with the electrochemical lateral-flow immunostrips for various concentrations of troponin I spiked in troponin I-free human serum. (b) Calibration plot: concentration dependence of the charge at 60 s in panel a. Each concentration experiment was carried out with three different immunostrips for the same sample. The data were subtracted by the mean value obtained from seven measurements, at zero concentration. The dashed line corresponds to 3 times the standard deviation (SD) of the charge at a concentration of zero. The error bars represent the SD of three measurements. (c) Chronocoulograms obtained with electrochemical lateral-flow immunostrips in serum containing either (i) 0  $\text{pg mL}^{-1}$  troponin I, (ii) 0  $\text{pg mL}^{-1}$  troponin I, 0.1  $\text{mM}$  AA, and 1  $\mu\text{g mL}^{-1}$  alkaline phosphatase (ALP), (iii) 1  $\text{pg mL}^{-1}$  troponin I, or (iv) 1  $\text{pg mL}^{-1}$  troponin I, 0.1  $\text{mM}$  AA and 1  $\mu\text{g mL}^{-1}$  ALP. (d) Histograms of the charges obtained for troponin I in serum containing only troponin I and in serum containing a standard troponin mixture, at concentrations of 1  $\text{pg mL}^{-1}$  and 1  $\text{ng mL}^{-1}$ .

the charge obtained with the standard reference material was similar to that obtained with troponin I at both concentrations (1  $\text{pg mL}^{-1}$  and 1  $\text{ng mL}^{-1}$ ). This result clearly shows that the concentration of troponin I in the study was reliable.

To evaluate the practical applicability, the lateral-flow immunoassay was tested with real clinical samples. The results for six clinical samples are shown in Table S1 of the ESI.† The calculated concentrations were mostly in good agreement with the concentrations measured with a commercial instrument, although the latter might also not be accurate, except for the higher values in two samples (samples 5 and 6). It is worthwhile to mention that troponin I in sample 1, though undetected with the commercial instrument, was detected with the lateral-flow immunoassay. These results show that the developed immunoassay could be applicable to the analysis of real clinical samples after further improvement.

## Conclusions

We have developed an ultrasensitive interference-free and rapid electrochemical lateral-flow immunoassay. With consideration

of pH dependence of ECC redox cycling, a novel combination of enzyme label, substrate, and product (Gal, AN-GP, and AN) enabled fast enzymatic reaction and ECC redox cycling by Gal and AN, respectively, in addition to a low background level in serum containing TCEP. The selective ECC redox cycling of AN allowed the negligible interference of electroactive species. A simple lateral-flow immunostrip including an asymmetric membrane pad and a patterned ITO working electrode was designed for efficient implementation of the assay. The total assay time was as short as 11 min. The calculated detection limit for troponin I ( $0.1 \text{ pg mL}^{-1}$ ), which is the lowest reported value in lateral-flow immunoassays, and the applicability of the assay for the detection of troponin I over a wide range of concentrations (from  $0.1 \text{ pg mL}^{-1}$  to  $100 \text{ ng mL}^{-1}$ ) together are conclusive of the fact that the proposed immunoassay is rapid, simple, and ultrasensitive. We believe that the present approach will open new avenues for developing simple and ultrasensitive POCT devices.

## Acknowledgements

This research was supported by the National Research Foundation of Korea (2010-0020772, 2012R1A2A2A06045327, 2012-M3C1A1-048860, and 2005-01333).

## Notes and references

- 1 V. Gubala, L. F. Harris, A. J. Ricco, M. X. Tan and D. E. Williams, *Anal. Chem.*, 2012, **84**, 487–515.
- 2 P. B. Lippa, C. Müller, A. Schlichtiger and H. Schlebusch, *Trends Anal. Chem.*, 2011, **30**, 887–898.
- 3 A. Warsinke, *Anal. Bioanal. Chem.*, 2009, **393**, 1393–1405.
- 4 G. A. Posthuma-Trumpie, J. Korf and A. van Amerongen, *Anal. Bioanal. Chem.*, 2009, **393**, 569–582.
- 5 D. Pyo and J. Yoo, *J. Immunoassay Immunochem.*, 2012, **33**, 203–222.
- 6 L. Gervais, N. de Rooij and E. Delamarche, *Adv. Mater.*, 2011, **23**, H151–H176.
- 7 D. Mark, S. Haeberle, G. Roth, F. von Stetten and R. Zengerle, *Chem. Soc. Rev.*, 2010, **39**, 1153–1182.
- 8 A. K. Yetisen, M. S. Akrama and C. R. Lowe, *Lab Chip*, 2013, **13**, 2210–2251.
- 9 A. W. Martinez, S. T. Phillips, G. M. Whitesides and E. Carrilho, *Anal. Chem.*, 2010, **82**, 3–10.
- 10 X. Mao, Y. Ma, A. Zhang, L. Zhang, L. Zeng and G. Liu, *Anal. Chem.*, 2009, **81**, 1660–1668.
- 11 D. H. Choi, S. K. Lee, Y. K. Oh, B. W. Bae, S. D. Lee, S. Kim, Y. B. Shin and M.-G. Kim, *Biosens. Bioelectron.*, 2010, **25**, 1999–2002.
- 12 J.-H. Cho, E.-H. Paek, I.-H. Cho and S.-H. Paek, *Anal. Chem.*, 2005, **77**, 4091–4097.
- 13 C. Fernández-Sánchez, C. J. McNeil, K. Rawson and O. Nilsson, *Anal. Chem.*, 2004, **76**, 5649–5656.
- 14 H. Yang, *Curr. Opin. Chem. Biol.*, 2012, **16**, 422–428.
- 15 M. R. Akanda, M. A. Aziz, K. Jo, V. Tamilavan, M. H. Hyun, S. Kim and H. Yang, *Anal. Chem.*, 2011, **83**, 3926–3933.
- 16 M. R. Akanda, Y. L. Choe and H. Yang, *Anal. Chem.*, 2012, **84**, 1049–1055.
- 17 M. R. Akanda, V. Tamilavan, S. Park, K. Jo, M. H. Hyun and H. Yang, *Anal. Chem.*, 2013, **85**, 1631–1636.
- 18 A. Singh, S. Park and H. Yang, *Anal. Chem.*, 2013, **85**, 4863–4868.
- 19 A. Dasgupta, L. Chow, A. Wells and P. Datta, *J. Clin. Lab. Anal.*, 2001, **15**, 175–177.
- 20 H.-A. Joung, Y. K. Oh and M.-G. Kim, *Biosens. Bioelectron.*, 2014, **53**, 330–335.
- 21 B. K. Kim, S. Y. Yang, M. A. Aziz, K. Jo, D. Sung, S. Jon, H. Y. Woo and H. Yang, *Electroanalysis*, 2010, **22**, 2235–2244.
- 22 Y. K. Oh, H.-A. Joung, S. Kim and M.-G. Kim, *Lab Chip*, 2013, **13**, 768–772.
- 23 M. Shi and F. C. Anson, *Langmuir*, 1996, **12**, 2068–2075.
- 24 J. Das, J.-A. Lee and H. Yang, *Langmuir*, 2010, **26**, 6804–6808.
- 25 W.-Z. Jia, K. Wang and X.-H. Xia, *Trends Anal. Chem.*, 2010, **29**, 306–318.
- 26 L. Wechtersbach and B. Cigić, *J. Biochem. Biophys. Methods*, 2007, **70**, 767–772.
- 27 J. Zhu, N. Zou, D. Zhu, J. Wang, Q. Jin, J. Zhao and H. Mao, *Clin. Chem.*, 2011, **57**, 1732–1738.
- 28 Q. Xu, H. Xu, H. Gu, J. Li, Y. Wang and M. Wei, *Mater. Sci. Eng., C*, 2009, **29**, 702–707.
- 29 J. Zhu, N. Zou, H. Mao, P. Wang, D. Zhu, H. Ji, H. Cong, C. Sun, H. Wang, F. Zhang, J. Qian, Q. Jin and J. Zhao, *Biosens. Bioelectron.*, 2013, **42**, 522–525.